Proceedings Paper:
Meng, W, Liu, Q, Zhang, M et al. (2017) Compliance adaptation of an intrinsically soft ankle rehabilitation robot driven by pneumatic muscles. In: 2017 IEEE International Conference on Advanced Intelligent Mechatronics (AIM 2017). AIM 2017, 03-07 Jul 2017, Munich, Germany. IEEE, pp. 82-87. ISBN: 978-1-5090-5998-0. ISSN: 2159-6255. EISSN: 2159-6255.

https://doi.org/10.1109/AIM.2017.8013999

Compliance Adaptation of An Intrinsically Soft Ankle Rehabilitation Robot Driven by Pneumatic Muscles*

Wei Meng, *Member, IEEE*, Quan Liu, Mingming Zhang, *Member, IEEE*, Qingsong Ai, and Sheng Quan Xie, *Senior Member, IEEE*

***Abstract*—Pneumatic muscles (PMs)-driven robots become more and more popular in medical and rehabilitation field as the actuators are intrinsically complaint and thus are safer for patients than traditional rigid robots. This paper proposes a new compliance adaptation method of a soft ankle rehabilitation robot that is driven by four pneumatic muscles enabling three rotational movement degrees of freedom (DoFs). The stiffness of a PM is dominated by the nominal pressure. It is possible to control the robot joint compliance independently of the robot movement in task space. The controller is designed in joint space to regulate the compliance property of the soft robot by tuning the stiffness of each active link. Experiments in actual environment were conducted to verify the control scheme and results show that the robot compliance can be adjusted when provided changing nominal pressures and the robot assistance output can be regulated, which provides a feasible solution to implement the patient-cooperative training strategy.**

***Index Terms*—Compliance adaptation, soft rehabilitation robot, pneumatic muscles, nominal pressure**

I. Introduction

China has an increasingly aged and stroke population, and as these demographics increase there are increased demand for rehabilitation but decreased availability of people who can deliver rehabilitation. The percentage of Chinese above the 60 is expected to reach 39% of the population by 2050 [1]. Age-related neurologic conditions, such as stroke, continue to be a major cause of morbidity in the world. In China, the annual stroke people is approximately 2 million, and stroke has become the leading cause of adult disability [2]. Due to the increases in numbers of elderly people and stroke survivors, the management of the long-term physical, emotional, and social consequences of stroke has become a major global issue. Robot-assisted solutions have the potential to alleviate the burden of post-stroke rehabilitation, transforming today's labor- intensive tasks into technology-assisted operations [3]. Rehabilitation robots have become the one of the most important solutions as adjunct to the physical therapists [4].

However, a majority of existing rehabilitation robots are driven by rigid and stiff actuators such as electric motors. In terms of ankle rehabilitation, the Anklebot (Interactive Motion Technologies, Inc., USA) [5] is a robot driven by two linear actuators mounted in parallel and can actuate two DoFs of ankle movement [6]. Saglia et al. presented an Ankle Rehabilitation roBOT (ARBOT) with two rotational DoFs driven by DC motors [7]. These stiff actuators along with trajectory tracking control scheme may produce large forces in response to the undesirable motions produced by position errors and may lead to secondary injuries to patients [8]. To tackle these problems, an impedance or admittance controller with proper stiffness and damping can be adopted to make the robot behaved with some compliant features [9, 10]. The paradigm of compliance adaptation is important in rehabilitation field to provide a soft and safe environment for the patients. Actually there have been some extensive work such as patient-cooperative or assist-as-needed strategy [11, 12] on Lokomat and LOPES [13, 14]. However, most of existing work are applied to traditional rigid robots. However, this attempt or provide compliant actuation may add an extra layer of control complexity to the robot controller.

It has been well-recognized that inherent compliance of robot will help realize the safe human robot interaction in rehabilitation. Pneumatic muscle is a promising intervention in the field of rehabilitation robotics due to its lightweight features and high power/weight, power/volume ratios. Hussain et al. [15] designed a lightweight orthosis driven by PMs, and an impedance control strategy was developed in task space to provide interactive robotic gait training. A knee-ankle-foot orthosis (KAFO) powered by PM with myoelectric (EMG) activation and inhibition was proposed by Sawicki et al. [16] Different from rigid robots, which can only provide "virtual" compliance as it only reflects the robot softness when it interacts with the environment, an advantage of the PMs-driven soft ones is that their actuators can provide variable compliance during operation. This variable actuation compliance is beneficial to make the robot being "real" soft.

It indicated that the actuation stiffness of PM would be influenced by the initial pressure but the relationship between them has not been fully investigated or modelled. Choi and Lee [17] presented a novel approach to control the compliance

*Research supported by National Natural Science Foundation of China under grants with no. 51675389 and no. 51475342.

W. Meng is with the School of Information Engineering, Wuhan University of Technology, Wuhan, China, and the Key Laboratory of Fiber Optic Sensing Technology and Information Processing (Wuhan University of Technology), Ministry of Education (e-mail: weimeng@whut.edu.cn).

Q. Liu is with the School of Information Engineering, Wuhan University of Technology, Wuhan, China, and the Key Laboratory of Fiber Optic Sensing Technology and Information Processing (Wuhan University of Technology), Ministry of Education (e-mail: quanliu@whut.edu.cn).

M. Zhang is with the Department of Mechanical Engineering, University of Auckland, Auckland, New Zealand (email: mzha130@aucklanduni.ac.nz)

Q. Ai is with the School of Information Engineering, Wuhan University of Technology, Wuhan, China, and the Key Laboratory of Fiber Optic Sensing Technology and Information Processing (Wuhan University of Technology), Ministry of Education (e-mail: qingsongai@whut.edu.cn).

S. Q. Xie is with the School of Electrical and Electronic Engineering and School of Mechanical Engineering, University of Leeds, UK, and the School of Information Engineering, Wuhan University of Technology, Wuhan, China (e-mail: s.q.xie@leeds.ac.uk).

and position independently for a pneumatic muscles actuated joint. However, the relation between pressure and robot stiffness and the pressure-based compliance control have not been reported in literature [18]. In this paper, a new compliance adaptation method using pressure adjustment is presented as first specific solution to provide compliance in joint space for a soft ankle rehabilitation robot. The proposed control scheme allows the robotic compliance to be controlled independently of the end effector position control.

Different from existing compliance control of the rehabilitation devices, in this paper it is achieved by directly influencing the nominal pressure of each actuator which will change inherent compliance of the soft ankle robot itself. If the nominal pressure is controlled to an increased level the low level of robot compliance can be achieved and thus a small movement deviation error can be guaranteed. On the contrary, the controller can increase the robot compliance by adopting a lower nominal pressure to allow more patient moving freedoms during robot-assisted exercise.

The rest of this paper is organized as follows: Section II demonstrates the PMs-driven soft ankle rehabilitation robot. In Section III, the proposed robot compliance model on the basis of joint nominal pressure is presented. Experiments of robots with human participants were conducted in Section IV, followed by the discussion and conclusion in Section V.

II. Soft Ankle Rehabilitation Robot

The current prototype of the soft ankle rehabilitation robot is shown in Fig. 1 [19, 20]. This robot is actuated by four active PM links in parallel to realize the three rotational DoFs of the ankle joint, including dorsiflexion/plantarflexion, inversion/ eversion, and adduction/abduction, respectively. The PMs with model FESTO DMSP-20-400N are adopted here to guarantee the intrinsic compliance of the robot when interacts with patients. High dynamic pneumatic regulator (FESTO VPPM-6L-L-1-G18-0L6H) is used to regulate the pressure inside each muscle. The end-effector is a three-link serial manipulator with three magnetic encoders (AMS AS5048A) embedded to provide measurements of angular positions of the robot in Euler X, Y and Z axes.

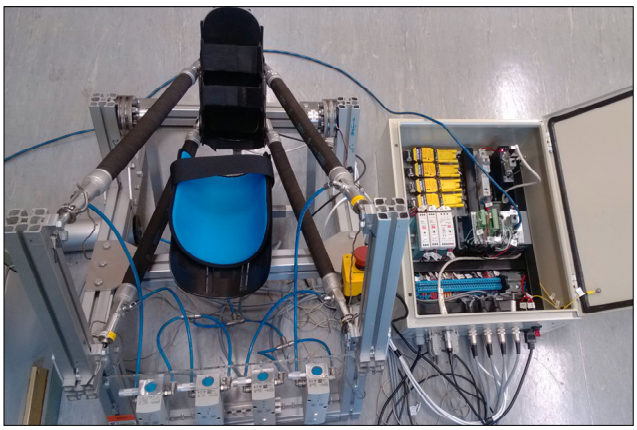

Figure 1. Prototype of the soft ankle rehabilitation robot.

In this study, we only concern the actuated DoFs in ankle dorsiflexion/ plantarflexion and inversion/ eversion while the adduction/abduction DoF will be kept passive and free. The rest length of each PM is 400*mm* with a maximum stroke 100*mm*. Each PMA can provide a peak 1000N pulling force, which is sufficient for the ankle stretching application. A single-axis tension load cell (Futek LCM 300) is placed in series with the PMA and a six-axis load cell (SRI M3715C) is mounted between the robot end-effector and the foot plate to measure the human-robot interaction torque. All the hardware was controlled by using a NI Compact RIO-9022 system and the control system run on a host PC using LabVIEW.

Kinematic model maps the relation between robot end-effector movement with the joint link displacements [21]. Define vector of each active link is L_i and it can be calculated by a given end effector orientation $\theta_{3\times1} = [\theta_x;\ \theta_y;\ \theta_z]$. Define P_i^f and P_i^m are the connection point vectors of the upper fixed platform and the lower moving platform, respectively, R_m^f is the rotational transformation matrix, the Jacobian matrix that relates the link velocities and the twist of the end effector, also the joint forces with the end effector torque, of which the i^{th} row can be expressed by:

$$J_i = \left(R_m^f P_i^m \times \frac{L_i}{l_i}\right)^T \tag{1}$$

where l_i is the link length, $l_i = \sqrt{{L_i}^T L_i}$. The element of Jacobian matrix $J_{4\times3}$ is

$$J_{i,j} = \frac{\partial l_i}{\partial \theta_j} = \frac{1}{l_i}\left(\frac{\partial R_m^f}{\partial \theta_j} P_i^m\right)^T \left(O_f O_r - P_i^f\right) \tag{2}$$

For kinematics analysis, it has:

$$\dot{l}_i = J\omega,\ F = J^{-T}\tau. \tag{3}$$

In which $\dot{l}_i$ is the joint velocity of each link, ω is the angular velocity of end effector, $F_{4\times1}$ is the link force and $\tau_{3\times1}$ is the produced end effector torque. By using Jacobian matrix the actuating force in joint space can be mapped to the force/moment of the moving platform in task space.

III. Compliance Modelling of the Robot via PM Nominal Pressure Adaptation

A. Modeling the PM

Pneumatic muscles are usually composed of internal cylindrical barrels of rubber and external rigid fiber braid. When the rubber tube inflates, the radial volume will expand, resulting in axial contraction force and thus pulling movement. In contrast, due to the elastic force of the rubber tube, the pneumatic muscles will gradually return to their original volume and length when deflating. A typical geometrical structure of the pneumatic muscles is shown in Fig. 2, in which the initial length l_0, the initial diameter D_0, initial fiber braided angle θ_0 are shown, and suppose that the actual length is l after contraction, the actual diameter D, and the actual fiber braided angle θ, the muscle contraction rate can be expressed as $\varepsilon = (l_0 - l)/l_0 = (cos\theta_0 - cos\theta)/cos\theta_0$.

The relationship between PM's air pressure P, the muscle contraction rate ε, and the external load F (can be considered as the produced pulling force) is expressed by (4).

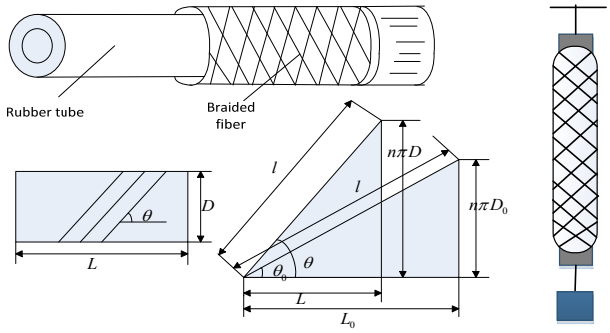

Figure 2. A typical geometrical structure of pneumatic muscles.

$$P = \frac{F}{a(1-\varepsilon)^2 - b} \tag{4}$$

where $a = (3\pi D_0^2)/(4tan^2\,\theta_0)$, $b = (\pi D_0^2)/(4sin^2\,\theta_0)$, then the contraction force F can be obtained by (5). Stiffness of a PM can be regarded as the output force caused by unit changes of PM's length like the following equation:

$$F = \frac{\pi D_0^2 P(3L^2 - b^2)}{4b^2} \tag{5}$$

$$K = \frac{\partial F}{\partial L} = \frac{6\pi D_0^2 PL}{4b^2} \tag{6}$$

Modelling of the robot with PMs was a crucial task as they exhibit highly nonlinear force-length characteristics. In this study, we considered the PM numerical model developed by Sarosi et al. [22], although other approaches to modelling also exist [23-25]. The function approximation proposed by Sarosi et al. is easy to apply to robots powered by PMs and is adopted here to derive the PM contraction force F based on its pressure inside p and contraction strain k, as shown in (7), in which the strain is expressed as the ratio of the contraction length to the initial length. We refer the reader to [22] for further details about the development of the PM model. In this research, the parameters a, b, c, d, e were experimentally obtained by changing the muscle length while the contraction force and pressure were recorded. Specifically, for inflation and deflation processes of the DMSP-20-400-RM-RM model can be expressed by (8) respectively.

$$F(p,k) = (p+a)e^{b\cdot k} + c\cdot p\cdot k + d\cdot p + e. \tag{7}$$

$$\begin{cases} F_{inf} = (p+232.89)e^{-38.32k} - 904.01pk + 294.86p - 289.06 \\ F_{def} = (p+272.70)e^{-32.58k} - 908.24pk + 298.83p - 262.85 \end{cases} \tag{8}$$

B. Robot Compliance Adaptation

The robot torque generated by the muscle actuators can be expressed by (9), where $F_{4\times1} = [F_1;\ F_2;\ F_3;\ F_4]$ is the vector of contraction forces generated by the four parallel PMs. The stiffness performance of the robot end effector when assisting human ankle can be expressed by (10), in which τ_{rob} is the function of J (decided by the robot angle θ, as in (1)) and F (determined by the muscle pressure p and the strain which is also dominated by the angle θ, as in (5)). From the equation we can assume that the robot stiffness K_{rob} and robot compliance C_{rob} has a close relation with the pressure inside each muscle. Unlike traditional antagonistically actuated joints, the robot here is driven by four muscles in parallel, which means the torque-stiffness and pressure relations are not as simple as the previously presented equations in [15, 17].

$$\tau_{rob} = J^T F = J^T[F_1, F_2, F_3, F_4]. \tag{9}$$

$$K_{rob} = \frac{\partial \tau_{rob}}{\partial \theta},\ C_{rob} = \frac{1}{K_{rob}} \tag{10}$$

In this research, we use function approximation method on the experiment results with various pressures to establish the relationship between robot end effector torque and angle and then derive the model for stiffness of the robot actuated by PMs. The experiments have been performed at low speeds (when reproducing pure stiffness) in order to avoid the effect of inertial torques and forces. Then the robot compliance can be obtained from the estimated stiffness such as (11), in which the superscript x, y represent the parameters are in ankle dorsiflexion/plantarflexion, inversion/ eversion respectively.

$$\begin{cases} K_{rob}^x(p) = k_{p1}^x p^3 + k_{p2}^x p^2 + k_{p3}^x p + k_{p4}^x \\ K_{rob}^y(p) = k_{p1}^y p^3 + k_{p2}^y p^2 + k_{p3}^y p + k_{p4}^y \end{cases}. \tag{11}$$

The objective of the compliance control law is to adjust the robot output based on the extent of the human subjects' active joint torque contribution. Thus, the adjustment of joint stiffness of the robot will, in turn, increase or decrease the amount of joint force and thus the assistance (τ_{rob}). The compliance property of the robot can be adapted by regulating the nominal pressure of the actuation muscles. The previous work using similar method only have been reported on the antagonistic muscles actuated robot [17], in which the joint compliance is easy to calculate. In this study, we used experiments and linear function approximation method to get the relationship between calculated robot torques and a sequence of pressures range from 2.6 bar to 4.0 bar (2.6 bar, 2.8 bar, 3.0 bar, 3.2 bar, 3.4 bar, 3.6 bar, 4.0 bar), then the robot stiffness can be obtained as a polynomial function of the nominal pressure inside muscles.

The modeling process of the robot compliance can be demonstrated by the following graphs plotted in Fig. 3. We first conduct three repetitive tests to gather the produced robot torque τ_{rob} and the robot movement trajectory θ data with different nominal pressures. Here we give three examples with pressure 2.6 bar, 3.4 bar, and 4.0 bar, respectively. The τ_{rob} is obtained from the real- time measured pulling force by using (12), and the stiffness K is then calculated using (13) together with linear approximation method once getting τ_{rob} and θ. After getting the seven pairs of pressure and stiffness, we can plot a function to fit the curve of stiffness K_{rob} and pressure p. Here we use a 3-order function to approximate the relation. As a result, the robot stiffness in Euler X axis can be expressed by $K_{rob}^x(p) = 0.8793p^3 - 7.1805p^2 + 20.6232p - 14.147$ and the same procedure is conducted on Euler Y axis we get $K_{rob}^y(p) = -0.628p^3 + 6.823p^2 - 22.5308p + 27.9075$.

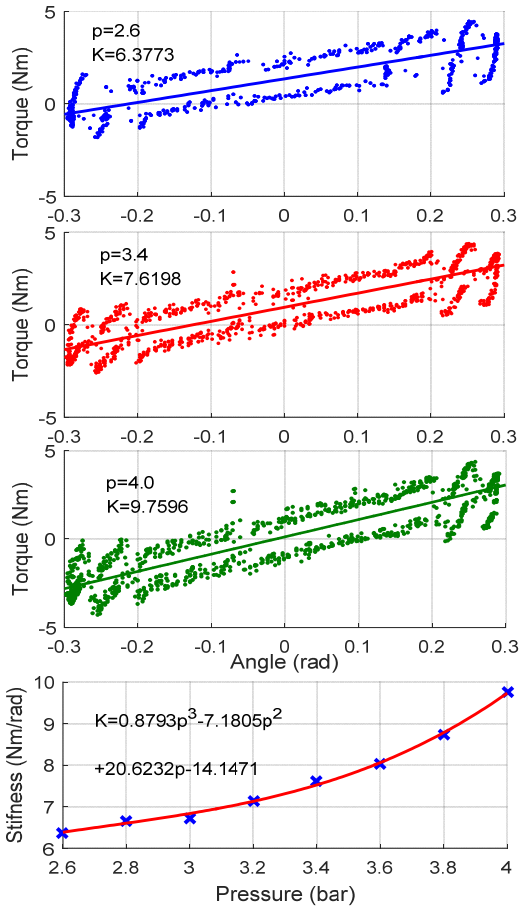

(a) the robot toque *vs* angle (to get stifness *K*) under different pressures and the robot stifness *vs* pressure in ankle dorsiflexion/plantarflexion axis

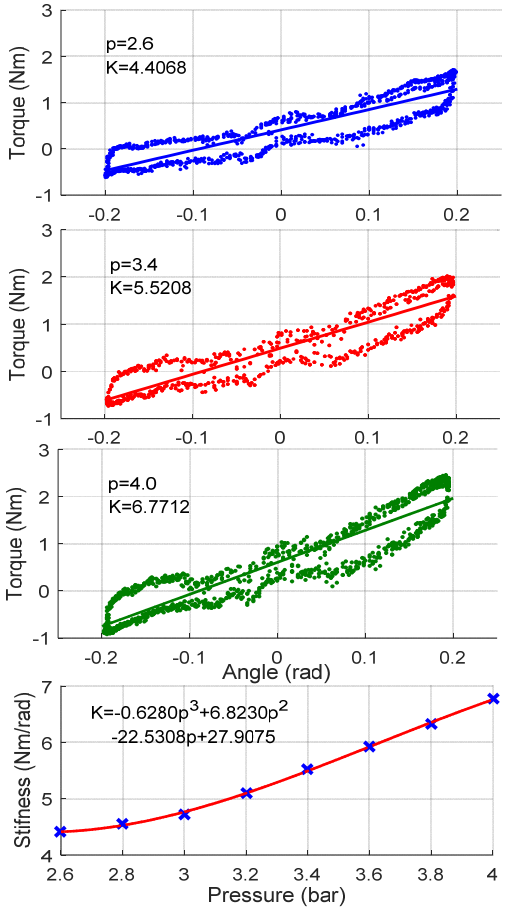

(b) the robot toque *vs* angle (to get stifness *K*) under different pressures and the robot stifness *vs* pressure in ankle inversion/ eversion axis

Figure 3. Relationship between end-effector stifness and nominal pressure.

IV. Experiments of Compliance Adaptation

The concept behind the adaptive compliance control is to set the robotic compliance low if little effort or participation is detected from the human subjects, which will increase the robotic assistance to guide the subjects' limbs on reference trajectories. Similarly, the compliance of the robot is adapted to a high level if the subjects show greater effort, which will allow more freedoms for the subject to deviate from reference trajectories. Such treatment strategy has been widely accepted by many clinical and engineering professionals [10, 26, 27].

The proposed adaptation control scheme of the robot compliance were evaluated on a human-ankle robot system. The experimental setup is presented in Fig. 4, where a healthy participant was sit on a height adjustable chair with his ankle-foot fixed on an orthosis that is mounted the end-effector. The goal of the experiments is to verify the general reaction of the compliance controller using the soft ankle rehabilitation robot to different pressure's behavior. A circle movement with dorsiflexion/plantarflexion and inversion/ eversion motions will be performed to show the influence of nominal pressure on the patient ankle-robot system. The reference trajectory is an ellipse with X amplitude of 0.22 rad and Y amplitude of 0.12 rad, and the robot was controlled for 80 seconds with a 0.05Hz frequency. Here we tried to test how the human-robot

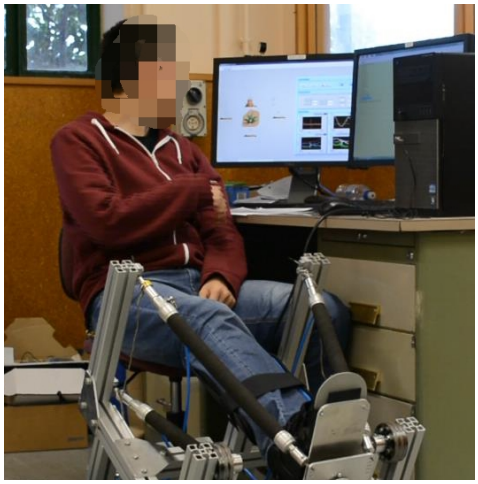

Figure 4. Experimental setup of the human-robot system.

interaction will be influenced by the robot compliance that is dominated by nominal pressure inside the pneumatic muscles of the joint space. Four different levels of nominal pressure were used: 0, 2.6 bar, 3.4 bar and 4.0 bar. The robot movement trajectories of the four tests with a healthy participant's ankle interaction effects are presented in the figures below.

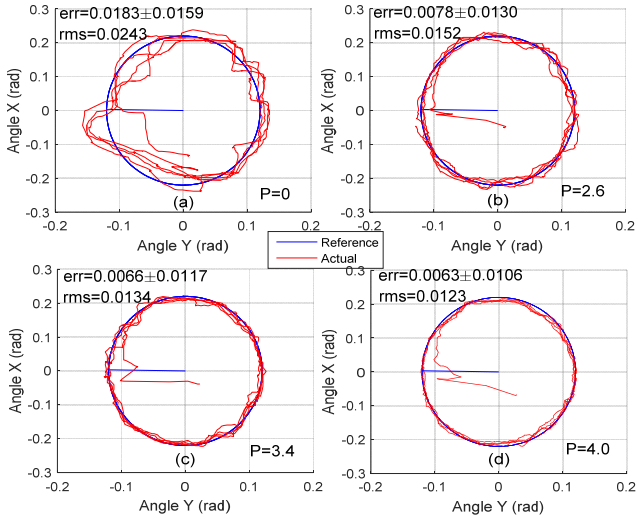

Figure 5. Human-robot movement under different compliance dominated by nominal pressures: (a) P=0, (b) P=2.6 bar, (c) P=3.4 bar and (d) P=4.0 bar.

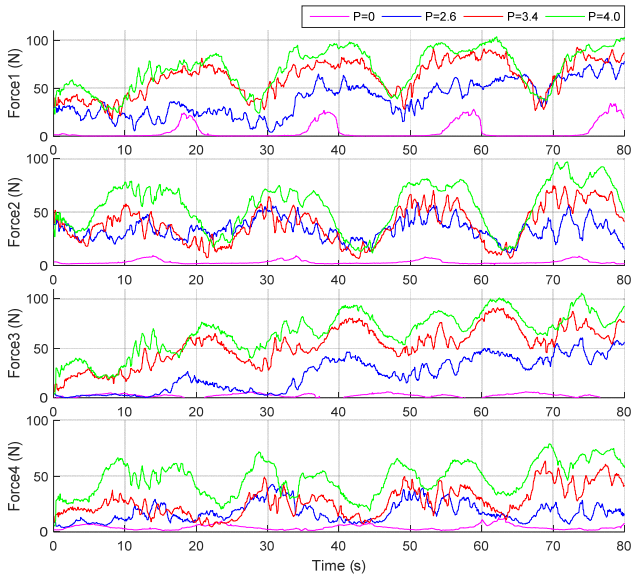

Figure 6. Robot joint actuation forces under different compliance dominate by different levels of nominal pressures.

In this paper, we developed a joint-space compliance adaptation scheme for an intrinsically soft ankle rehabilitation robot powered by PMs. The ankle-robot movement reaction to different nominal pressure is presented in Fig. 5, shown are average errors and standard deviations of four experiments with same external reference trajectory tracking conditions. The deviation levels were identified by calculating the Euclidian distance (error) between the measured position and the reference profile. The mean error and root mean square (RMS) represents a quantitative estimate whether the robot is more likely to be in a compliant state, with a large deviation or in a stiff state, with a small deviation. From Fig. 3 we found that the robot stiffness became higher when the nominal pressure increased and thus the compliance is lower. When the robot is fully compliant with 0 nominal pressure, the patient is completely free to move the end-effector along the reference trajectory, however the average tracking error and error RMS is the highest, i.e., 0.0183 rad and 0.0243 rad, respectively.

As the increase of robot stiffness as well as the reduction of robot compliance, the patient ankle's deviation freedom from the reference path became smaller, which can also be reflected by the better trajectory results with tracking errors 0.0078 rad, 0.0066 rad and 0.0063 rad for the three different levels of softness, respectively. At the same time, the error RMS was also reduced, and this help to conclude that the robot compliance is becoming lower and the robot assistance is high. From Fig. 6 we can see that with the increase of nominal pressure inside each PM, where purple, blue, red and green lines represent the pulling forces of pressures from 0 to 4.0 bar, respectively, the pulling force generated was higher and higher, which means the robot contributed more efforts during the operation. Thus, an adaptive compliance controller can be proposed to adjust the robotic compliance in response to the patient's action, by using the nominal pressure adaptation law.

V. Discussion and Conclusion

Furthermore, we investigated a joint-level compliance adaptation strategies that aim to adjust the robot's stiffness when interacting with participants during the robotic therapy. This compliance strategy modified the robot assistance output and based on the pneumatic muscles' nominal pressure. A key aspect of the control scheme lies in its joint space level of compliance adaptation. This formulation, unlike previous impedance-based control strategies, changing the amount of assistance by modifying the parameters of the impedance model [4, 28]. The proposed adaptation scheme presents an advancement on the current compliance control schemes of compliant actuators by adjusting the stiffness of the actuators themselves. Experimental results obtained on a human-robot system showed the effectiveness of the proposed pressure-regulated compliance adaptation method. By means of these changes in compliant actuators' stiffness, we hope to increase the controllability and effectiveness of soft and safe devices designs for human–robot interactive rehabilitation.

In this paper, we proposed and evaluated a new compliance adaptation strategy for the soft ankle rehabilitation robot that is actuated by four parallel PMs. A low-level compliance control is implemented by regulating the robot nominal pressure in joint space. Experiments were conducted on a human-robot system and the results show that the proposed compliance adaptation strategy can adjust the robot assistance level and change the patient's moving freedom to complete circle trajectory tracking tasks. The adaptive compliance control scheme can learn in real time the human subject's training requirement and adapts the nominal pressure inside each PM accordingly. In the future, a two-level compliance control strategy in both joint space and task space will be designed and evaluated. Also, rigorous clinical trials with neurologically impaired subjects are necessary to establish the therapeutic efficacy of the adaptive control scheme. This work will also help in further developing adaptive control schemes for robot powered by compliant actuators.

ACKNOWLEDGMENT

This research is funded by the National Natural Science Foundation of China (No. 51675389 and No. 51475342).

REFERENCES

[1] United Nations, "World Population Ageing - the United Nations," http://www.un.org/en/development/desa/population/publications/pdf/ageing/WPA2015_Report.pdf, 2016.

[2] L. Liu, D. Wang, K. L. Wong, and Y. Wang, "Stroke and stroke care in China," *Stroke*, vol. 42, pp. 3651-3654, 2011.

[3] W. Meng, Q. Liu, Z. Zhou, Q. Ai, B. Sheng, and S. Xie, "Recent development of mechanisms and control strategies for robot-assisted lower limb rehabilitation," *Mechatronics*, vol. 31, pp. 132-145, 2015.

[4] A. A. Blank, J. A. French, A. U. Pehlivan, and M. K. O'Malley, "Current trends in robot-assisted upper-limb stroke rehabilitation: promoting patient engagement in therapy," *Current physical medicine and rehabilitation reports*, vol. 2, pp. 184-195, 2014.

[5] J. C. P. Ibarra, W. M. dos Santos, H. I. Krebs, and A. A. Siqueira, "Adaptive impedance control for robot-aided rehabilitation of ankle movements," in *Biomedical Robotics and Biomechatronics (2014 5th IEEE RAS & EMBS International Conference on*, 2014, pp. 664-669.

[6] A. Roy, H. I. Krebs, J. E. Barton, R. F. Macko, and L. W. Forrester, "Anklebot-assisted locomotor training after stroke: A novel deficit-adjusted control approach," in *Robotics and Automation (ICRA), 2013 IEEE International Conference on*, 2013, pp. 2175-2182.

[7] J. A. Saglia, N. G. Tsagarakis, J. S. Dai, and D. G. Caldwell, "Control strategies for patient-assisted training using the ankle rehabilitation robot (ARBOT)," *IEEE/ASME Transactions on Mechatronics*, vol. 18, pp. 1799-1808, 2013.

[8] S. Hussain, S. Q. Xie, and P. K. Jamwal, "Control of a robotic orthosis for gait rehabilitation," *Robotics and Autonomous Systems*, vol. 61, pp. 911-919, 2013.

[9] L. Z. Pan, A. G. Song, G. Z. Xu, H. J. Li, H. Zeng, and B. G. Xu, "Safety Supervisory Strategy for an Upper-Limb Rehabilitation Robot Based on Impedance Control," *International Journal of Advanced Robotic Systems*, vol. 10, Feb 2013.

[10] P. K. Jamwal, S. Hussain, M. H. Ghayesh, and S. V. Rogozina, "Impedance Control of an Intrinsically Compliant Parallel Ankle Rehabilitation Robot," *IEEE Transactions on Industrial Electronics*, vol. 63, pp. 3638-3647, 2016.

[11] U. Keller, G. Rauter, and R. Riener, "Assist-as-needed path control for the PASCAL rehabilitation robot," in *Rehabilitation Robotics (ICORR), 2013 IEEE International Conference on*, 2013, pp. 1-7.

[12] M. Shahbazi, S. F. Atashzar, M. Tavakoli, and R. Patel, "Robotics-Assisted Mirror Rehabilitation Therapy: A Therapist-in-the-Loop Assist-as-Needed Architecture." *IEEE/ASME Transactions on Mechatronics*, vol. 21, pp. 1954-1965, 2016.

[13] M. Bernhardt, M. Frey, G. Colombo, and R. Riener, "Hybrid force-position control yields cooperative behaviour of the rehabilitation robot LOKOMAT," in *Proceedings of the 2005 IEEE 9th International Conference on Rehabilitation Robotics*, 2005, pp. 536-539.

[14] E. H. F. Van Asseldonk, R. Ekkelenkamp, J. F. Veneman, F. C. T. Van der Helm, H. van der Kooij, and Ieee, "Selective control of a subtask of walking in a robotic gait trainer(LOPES)," in *2007 IEEE 10th International Conference on Rehabilitation Robotics*, Vols 1 and 2, ed, 2007, pp. 841-848.

[15] S. Hussain, S. Q. Xie, and P. K. Jamwal, "Adaptive Impedance Control of a Robotic Orthosis for Gait Rehabilitation," *IEEE Transactions on Cybernetics*, vol. 43, pp. 1025-1034, Jun 2013.

[16] G. Sawicki and D. Ferris, "A pneumatically powered knee-ankle-foot orthosis (KAFO) with myoelectric activation and inhibition," *Journal of NeuroEngineering and Rehabilitation*, vol. 6, p. 23, 2009.

[17] T.-Y. Choi and J.-J. Lee, "Control of manipulator using pneumatic muscles for enhanced safety," *IEEE Transactions on Industrial Electronics*, vol. 57, pp. 2815-2825, 2010.

[18] T. Noritsugu, "Wearable power assist robot driven with pneumatic rubber artificial muscles," *Technological Advancements in Biomedicine for Healthcare Applications*, p. 139, 2012.

[19] M. Zhang, "Improving Effectiveness of Robot-Assisted Ankle Rehabilitation Via Biomechanical Assessment and Interaction Control," *University of Auckland*, 2016.

[20] W. Meng, S. Q. Xie, Q. Liu, C. Z. Lu, and Q. Ai, "Robust iterative feedback tuning control of a compliant rehabilitation robot for repetitive ankle training," *IEEE/ASME Transactions on Mechatronics*, vol. 22, pp. 173-184, 2017.

[21] M. Zhang, J. Cao, G. Zhu, Q. Miao, X. Zeng, and S. Q. Xie, "Reconfigurable workspace and torque capacity of a compliant ankle rehabilitation robot (CARR)," *Robotics and Autonomous Systems*, 2017.

[22] J. Sarosi, I. Biro, J. Nemeth, and L. Cveticanin, "Dynamic modeling of a pneumatic muscle actuator with two-direction motion," *Mechanism and Machine Theory*, vol. 85, pp. 25-34, 2015.

[23] D. B. Reynolds, D. W. Repperger, C. A. Phillips, and G. Bandry, "Modeling the dynamic characteristics of pneumatic muscle," *Annals of Biomedical Engineering*, vol. 31, pp. 310-317, 2003.

[24] C. Song, S. Xie, Z. Zhou, and Y. Hu, "Modeling of pneumatic artificial muscle using a hybrid artificial neural network approach," *Mechatronics*, 2015.

[25] B. Tondu and P. Lopez, "Modeling and control of McKibben artificial muscle robot actuators," *Control Systems, IEEE*, vol. 20, pp. 15-38, 2000.

[26] K. Michmizos, S. Rossi, E. Castelli, P. Cappa, and H. Krebs, "Robot-Aided Neurorehabilitation: A Pediatric Robot for Ankle Rehabilitation," *IEEE Transactions on Neural Systems & Rehabilitation Engineering*, vol. 23, pp. 1056-1067, 2015.

[27] A. U. Pehlivan, D. P. Losey, and M. K. O'Malley, "Minimal Assist-as-Needed Controller for Upper Limb Robotic Rehabilitation," *IEEE Transactions on Robotics*, vol. 32, pp. 113-124, 2016.

[28] W. Meng, Q. Liu, Z. Zhou, and Q. Ai, "Active interaction control applied to a lower limb rehabilitation robot by using EMG recognition and impedance model," *Industrial Robot: An International Journal*, vol. 41, pp. 465-479, 2014/08/12 2014.